Scientific Reports

Supplementary Information

# Structural mechanism of JH delivery in hemolymph by JHBP of silkworm, *Bombyx mori*

Rintaro Suzuki[1], Zui Fujimoto[1], Takahiro Shiotsuki[2], Wataru Tsuchiya[1], Mitsuru Momma[1], Akira Tase[1], Mitsuhiro Miyazawa[3] & Toshimasa Yamazaki[1*]

[1]*Biomolecular Research Unit, National Institute of Agrobiological Sciences, 2-1-2 Kannondai, Tsukuba, Ibaraki 305-8602, Japan*

[2]*Insect Growth Regulation Research Unit, National Institute of Agrobiological Sciences, 1-2 Owashi, Tsukuba, Ibaraki 305-8634, Japan*

[3]*Insect Mimetics Research Unit, National Institute of Agrobiological Sciences, 1-2 Owashi, Tsukuba, Ibaraki 305-8634, Japan*

[*]Correspondence and requests for materials should be addressed to T.Y. (tyamazak@nias.affrc.go.jp).

This Supplementary Information contains five figures and four tables.

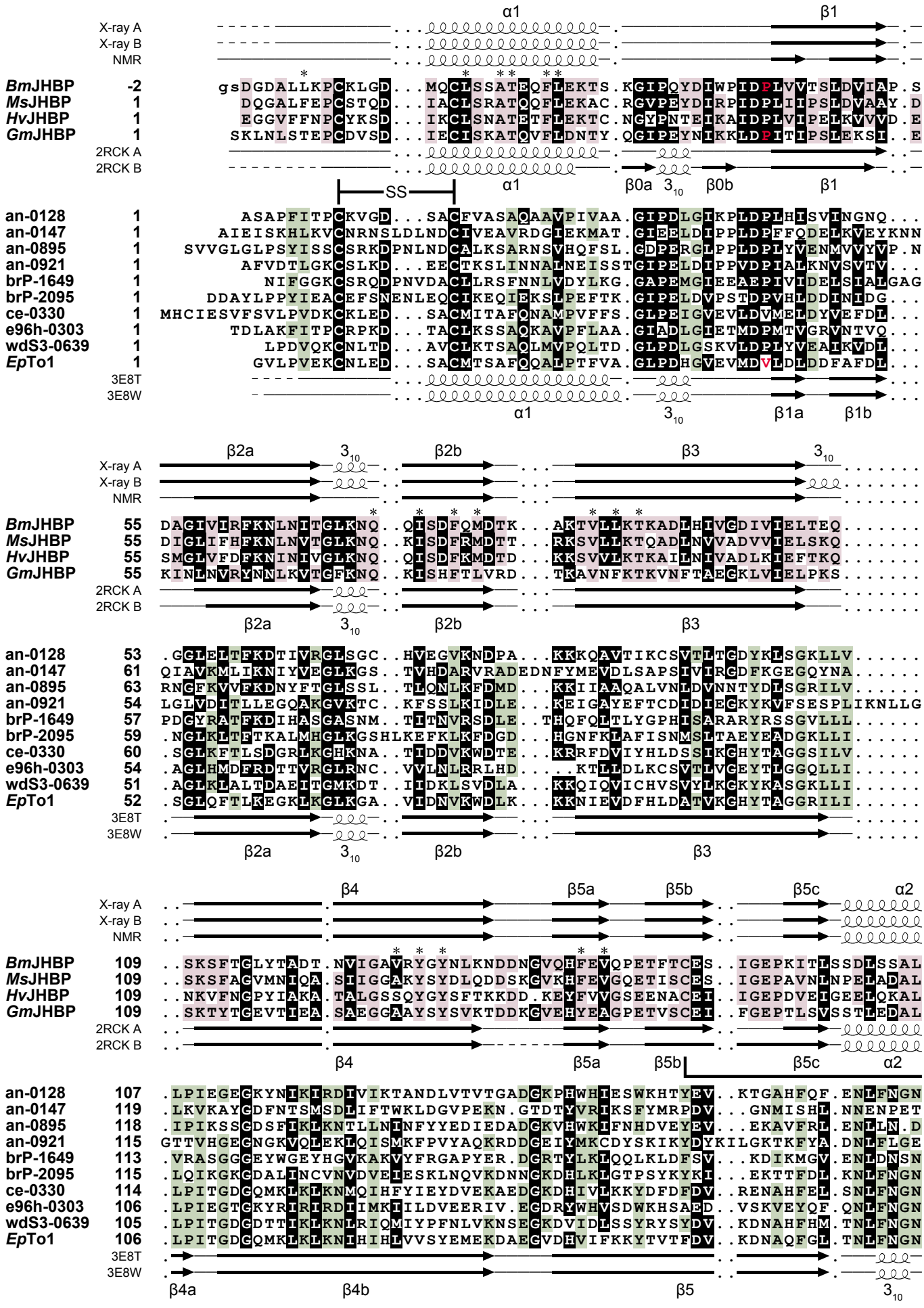
α1
β1
X-ray A
X-ray B
NMR
BmJHBP -2 gsDGDALLKPCKLGD...MQCLSSATEQFLEKTS.KGIPQYDIWPIDPLVVTSLDVIAP.S
MsJHBP 1 DQGALFEPCSTQD...IACLSRATQQFLEKAC.RGVPEYDIRPIDPLIIPSLDVAAY.D
HvJHBP 1 EGGVFFNPCYKSD...IKCLSNATETFLEKTC.NGYPNTEIKAIDPLVIPELKVVVD.E
GmJHBP 1 SKLNLSTEPCDVSD...IECISKATQVFLDNTY.QGIPEYNIKKLDPITIPSLEKSI..E
2RCK A
2RCK B
SS
α1
β0a
3₁₀
β0b
β1
an-0128 1 ASAPFITPCKVGD...SACFVASAQAAVPIVAA.GIPDLGIKPLDPLHISVINGNQ...
an-0147 1 AIEISKHLKVCNRNSLDLNDCIVEAVRDGIEKMAT.GIEELDIPPLDPFFQDELKVEYKNN
an-0895 1 SVVGLGLPSYISSCSRKDPNLNDCALKSARNSVHQFSL.GDPERGLPPLDPLYVENMVVYVP.N
an-0921 1 AFVDTLGKCSLKD...EECTKSLINNALNEISSTGIPELDIPPVDPIALKNVSVTV...
brP-1649 1 NIFGGKCSRQDPNVDACLLRSFNNLVDYLKG.GAPEMGIEEAEPIVIDELSIALGAG
brP-2095 1 DDAYLPPYIEACEFSNENLEQCIKEQIEKSLPEFTK.GIPELDVPSTDPVHLDDINIDG...
ce-0330 1 MHCIESVFSVLPVDKCKLED...SACMITAFQNAMPVFFS.GLPEIGVEVLDVMELDYVEFDL...
e96h-0303 1 TDLAKFITPCRPKD...TACLKSSAQKAVPFLAA.GIADLGIETMDPMTVGRVNTVQ...
wdS3-0639 1 LPDVQKCNLTD...AVCLKTSAQLMVPQLTD.GLPDLGSKVLDPLYVEAIKVDL...
EpTo1 1 GVLPVEKCNLED...SACMTSAFQQALPTFVA.GLPDHGVEVMDVLDLDDFAFDL...
3E8T
3E8W
α1
3₁₀
β1a
β1b
β2a
3₁₀
β2b
β3
3₁₀
X-ray A
X-ray B
NMR
BmJHBP 55 DAGIVIRFKNLNITGLKNQ..QISDFQMDTK...AKTVLLKTKADLHIVGDIVIELTEQ.....
MsJHBP 55 DIGLIFHFKNLNVTGLKNQ..KISDFRMDTT...RKSVLLKTQADLNVVADVVIELSKQ.....
HvJHBP 55 SMGLVFDFKNINIVGLKNQ..QISDFKMDTD...KKSVVLKTKAILNIVADLKIEFTKQ.....
GmJHBP 55 KINLNVRYNNLKVTGFKNQ..KISHFTLVRD...TKAVNFKTKVNFTAEGKLVIELPKS.....
2RCK A
2RCK B
β2a
3₁₀
β2b
β3
an-0128 53 .GGLELTFKDTIVRGLSGC..HVEGVKNDPA...KKKQAVTIKCSVTLTGDYKLSGKLLV.....
an-0147 61 QIAVKMLIKNIYVEGLKGS..TVHDARVRADEDNFYMEVDLSAPSIVIRGDFKGEGQYNA.....
an-0895 63 RNGFKVVFKDNYFTGLSSL..TLQNLKFDMD...KKIIAAQALVNLDVNNTYDLSGRILV.....
an-0921 54 LGLVDITLLEGQAKGVKTC..KFSSLKIDLE...KEIGAYEFTCDIDIEGKYKVFSESPLIKNLLG
brP-1649 57 PDGYRATFKDIHASGASNM..TITNVRSDLE..THQFQLTLYGPHISARARYRSSGVLLL.....
brP-2095 59 .NGLKLTFTKALMHGLKGSHLKEFKLKFDGD...HGNFKLAFISNMSLTAEYEADGKLLI.....
ce-0330 60 .SGLKFTLSDGRLKGHKNA..TIDDVKWDTE....KRRFDVIYHLDSSIKGHYTAGGSILV.....
e96h-0303 54 .AGLHMDFRDTTVRGLRNC..VVLNLRRLHD....KTLLDLKCSVTLVGEYTLGGQLLI.....
wdS3-0639 51 .AGLKLALTDAEITGMKDT..IIDKLSVDLA...KKQIQVICHVSVYLKGKYKASGKLLI.....
EpTo1 52 .SGLQFTLKEGKLKGLKGA..VIDNVKWDLK...KKNIEVDFHLDATVKGHYTAGGRILI.....
3E8T
3E8W
β2a
3₁₀
β2b
β3
β4
β5a
β5b
β5c
α2
X-ray A
X-ray B
NMR
BmJHBP 109 ..SKSFTGLYTADT.NVIGAVRYGYNLKNDDNGVQHFEVQPETFTCES..IGEPKITLSSDLSSAL
MsJHBP 109 ..SKSFAGVMNIQA.SIIGGAKYSYDLQDDSKGVKHFEVGQETISCES..IGEPAVNLNPEIADAL
HvJHBP 109 ..NKVFNGPYIAKA.TALGSSQYGYSFTKKDD.KEYFVVGSEENACEI..IGEPDVEIGEELQKAL
GmJHBP 109 ..SKTYTGEVTIEA.SAEGGAAYSYSVKTDDKGVEHYEAGPETVSCEI..FGEPTLSVSSTLEDAL
2RCK A
2RCK B
β4
β5a
β5b
β5c
α2
an-0128 107 .LPIEGEGKYNIKIRDIVIKTANDLVTVTGADGKPHWHIESWKHTYEV..KTGAHFQF.ENLFNGN
an-0147 119 .LKVKAYGDFNTSMSDLIFTWKLDGVPEKN.GTDTYVRIKSFYMRPDV...GNMISHL.NNENPET
an-0895 118 .IPIKSSGDSFIKLKNTLLNINFYYEDIEDADGKVHWKIFNHDVEYEV...EKAVFRL.ENLLN.D
an-0921 115 GTTVHGEGNGKVQLEKLQISMKFPVYAQKRDDGEIYMKCDYSKIKYDYKILGKTKFYA.DNLFLGE
brP-1649 113 .VRASGGGEYWGEYHGVKAKVYFRGAPYER.DGRTYLKLQQLKLDFSV...KDIKMGV.ENLDNSN
brP-2095 115 .LQIKGKGDALINCVNVDVEIESKLNQVKDNNGKDHLKLGTPSYKYKI...EKTTFDL.KNLFNGN
ce-0330 114 .LPITGDGQMKLKLKNMQIHFYIEYDVEKAEDGKDHIVLKKYDFDFDV..RENAHFEL.SNLFNGN
e96h-0303 106 .LPIEGTGKYRIRIRDIIMKILDVEERIV.EGDRYWHVSDWKHSAED..VSKVEYQF.QNLFNGN
wdS3-0639 105 .LPITGDGDTTIKLKNLRIQMIYPFNLVKNSEGKDVIDLSSYRYSYDV..KDNAHFHM.TNLFNGN
EpTo1 106 .LPITGDGQMKLKLKNIHIHLVVSYEMEKDAEGVDHVIFKKYTVTFDV..KDNAQFGL.TNLFNGN
3E8T
3E8W
β4a
β4b
β5
3₁₀

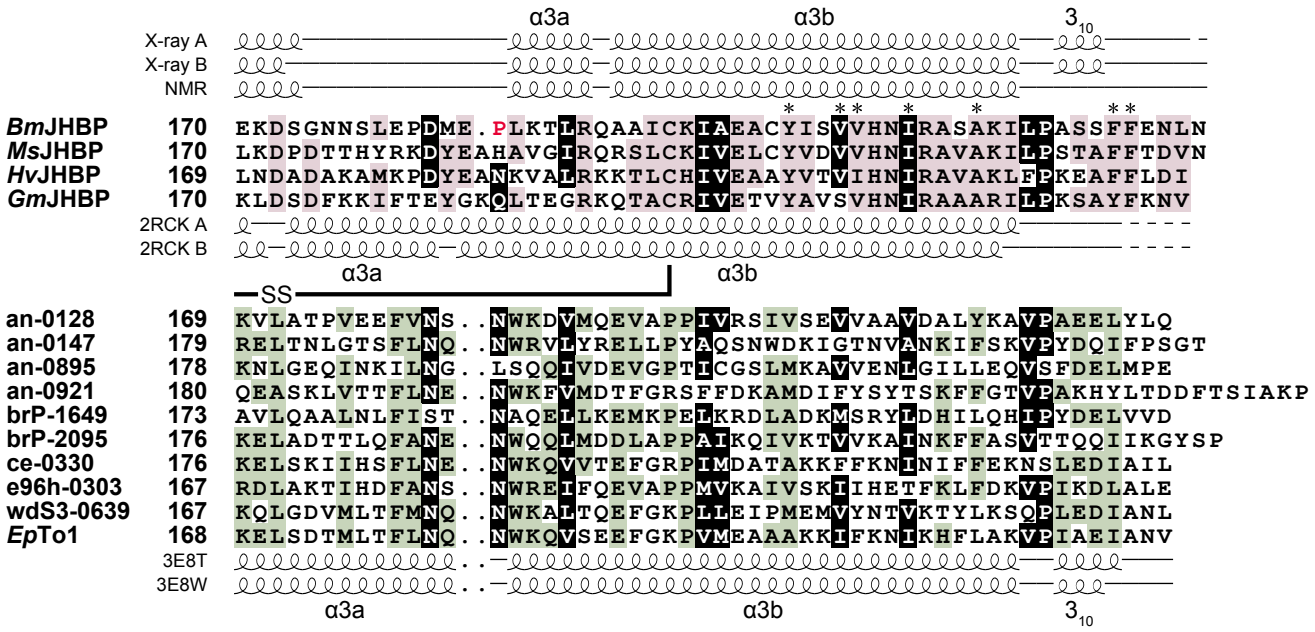


**Supplementary Figure S1 | Sequence alignment of JHBP/Takeout family.** *Bm*JHBP, *Ms*JHBP, *Hv*JHBP, and *Gm*JHBP denote JHBP of *Bombyx mori*, *Manduca sexta*, *Heliothis virescens*, and *Galleria mellonella*, respectively. *Ep*To1 denotes *Epiphyas postvittana* Takeout protein. Other nine sequences are deduced for *Bombyx mori* Takeout proteins reported previously (*13*). Secondary structure elements of *Bm*JHBP complexed with JH II in the crystalline state (X-ray) and with JH III in solution (NMR) are shown above its sequence while those of *Gm*JHBP (*15*) and *Ep*To1 (*14*) in the crystalline states are shown below their sequences. Residues colored red assume *cis* configuration in their three-dimensional structures. Highlighted in black backgrounds are residues strictly conserved and semiconserved for both the JHBP and Takeout subfamilies. Residues highlighted in purple and green backgrounds are conserved for the JHBP and the Takeout subfamily, respectively. The *Bm*JHBP residues essential for JH binding are indicated by asterisks (*) above its sequence. Alignment of multiple sequences and structures was initially achieved by the program MAFFTash (http://sysimm.ifrec.osaka-u.ac.jp/MAFFTash.3/) and modified manually so that the secondary structures are well-aligned and most gaps are located within loops.

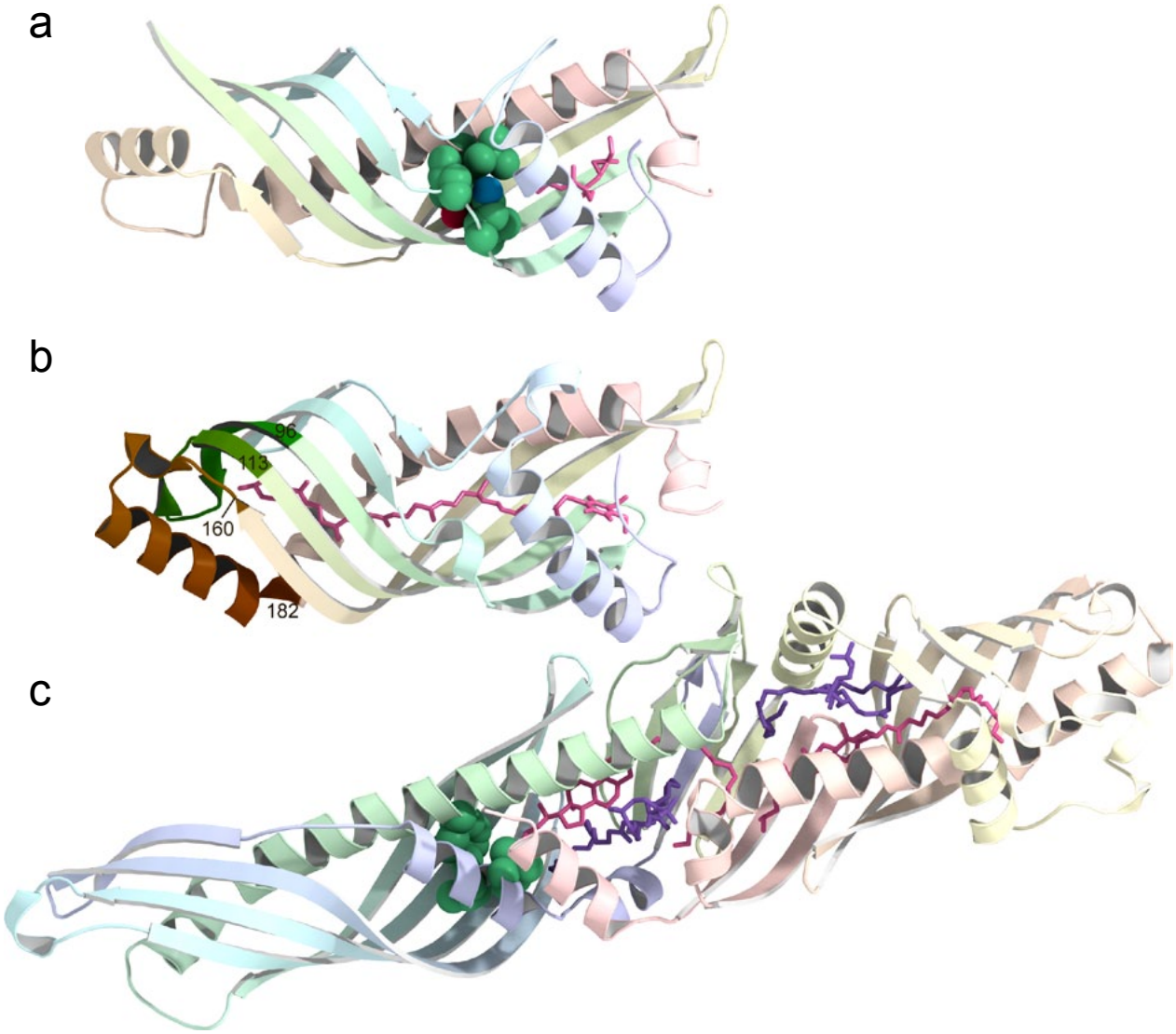


**Supplementary Figure S2 | Comparison of (a) the crystal structure of the gate-closed conformation of the *Bonbyx mori* JHBP in complex with JH II with reported crystal structures of (b) *Epiphyas postvittana* Takeout protein (*Ep*To1) (PDB ID: 3E8T) and (c) human cholesteryl ester transfer protein (CETP) (PDB ID: 2OBD).** JHBP and *Ep*To1 are displayed with the same orientation after three-dimensional superposition. CETP is displayed so as to show maximum similarity of its N-terminal domain with JHBP. Bound ligands are shown in stick models. Internal hydrophobic cavities of JHBP and the N-terminal domain of CETP are divided into two smaller pockets at the middle by hydrogen-bonded side chains and by hydrophobic side chains, respectively. These residues are shown as space filling structures. In the *Ep*To1 structure, Takeout-specific region composed of motif 1 (residues 96-113) and motif 2 (160-182) is highlighted.

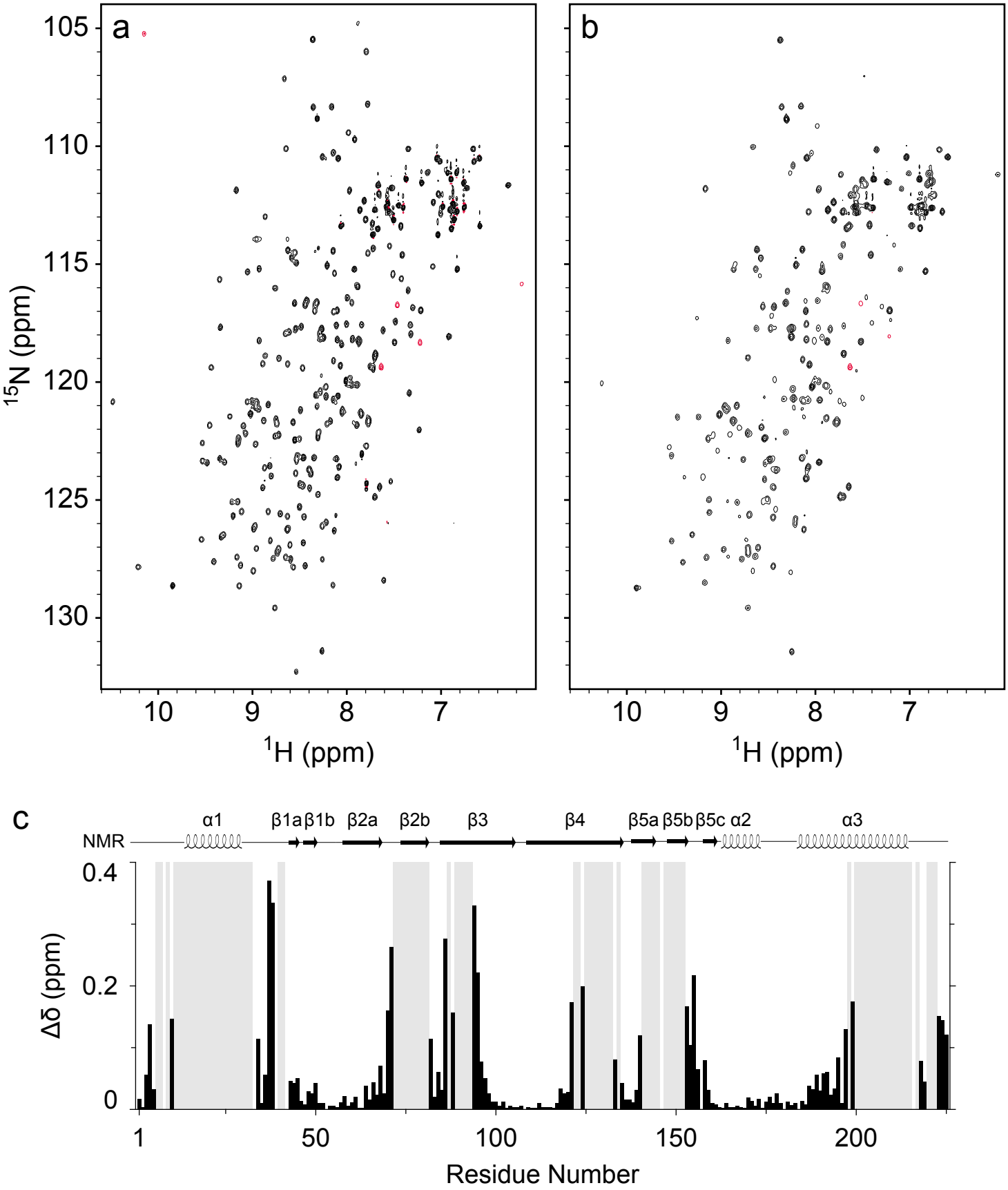


**Supplementary Figure S3 |** $^{1}$H-$^{15}$N HSQC spectra of (**a**) JH III-bound and (**b**) apo-JHBP in 45 mM sodium phosphate buffer, pH 6, collected at 35 °C on a Bruker DMX 750 spectrometer. Signals shown in red are folded under the experimental conditions employed. (**c**) Changes in backbone $^{1}$H and $^{15}$N chemical shifts of JHBP upon complex formation with JH III. Weighted chemical shift

differences between the apo- and JH III-bound JHBP, calculated with a function $\Delta\delta = [\Delta\delta_{HN}^{2} + (\Delta\delta_{15N}/5)^2]^{1/2}$, are shown against residue number. No NMR signals were observed for the shaded regions of the protein in the apo-form. The secondary structure elements of the JH III-bound form in solution are presented at the top of the figure.

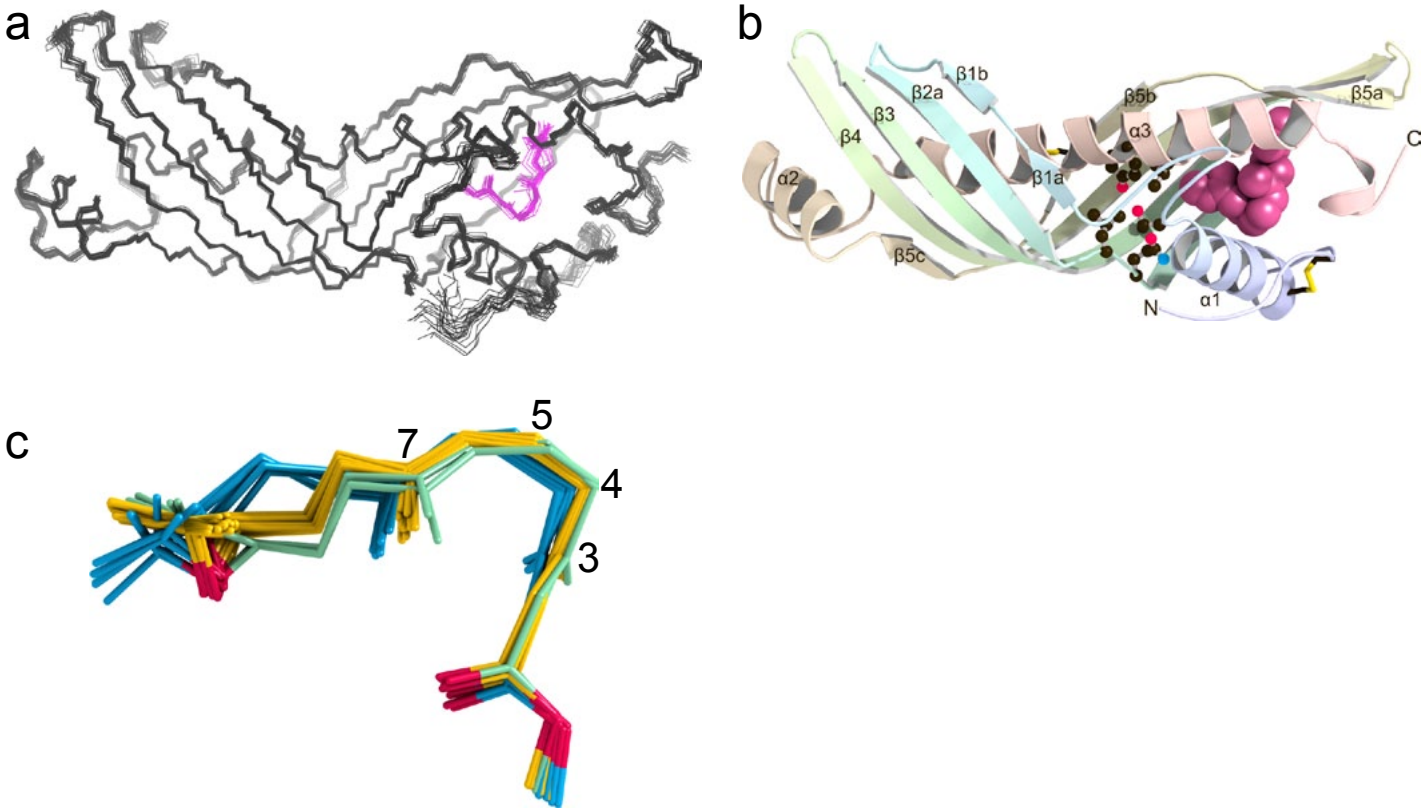


**Supplementary Figure S4 | NMR solution structures of *B. mori* JHBP-JH III complex.** (**a**) Superimposed backbone (N, $C^{\alpha}$ and C') atoms of the final 20 NMR-derived structures with the lowest energies for the JHBP-JH III complex. The backbone coordinates were superimposed against the representative structure, which showed minimum rmsd with the mean structure, using residues 1-225. JH III atoms are shown in pink. (**b**) A ribbon representation of the representative structure of the complex. Side chains of the residues forming the bottom wall of the JH-binding pocket are shown as ball-and-stick models and disulfide bonds as stick models. The bound-JH III molecule (pink) is depicted as a space-filling structure. (**c**) Superposition of the JHBP-bound JH III in solution. The observed L-shaped structures and crankshaft-like motions of the bound JH III in solution are similar to those for the bound JH II in the crystalline state (Figure 2C). Note that these L-shaped structures are accomplished by *gauche*(-) conformations about the C3-C4 and C4-C5 bonds instead of the successive *gauche*(+) conformations observed for the JHBP-bound JH II in the crystalline state. For the isolated JH III, conformational energies of the L-shaped structures with *gauche*(+) conformations and with *gauche*(-) conformations are comparable as calculated using the CHARMm force field (Supplementary Table S4). Nearly isoenergetic L-shaped structures in rapid equilibrium on the NMR time scale would make a favorable entropic contribution to complex formation. These findings suggest that JH has a certain motional freedom even when bound to JHBP.

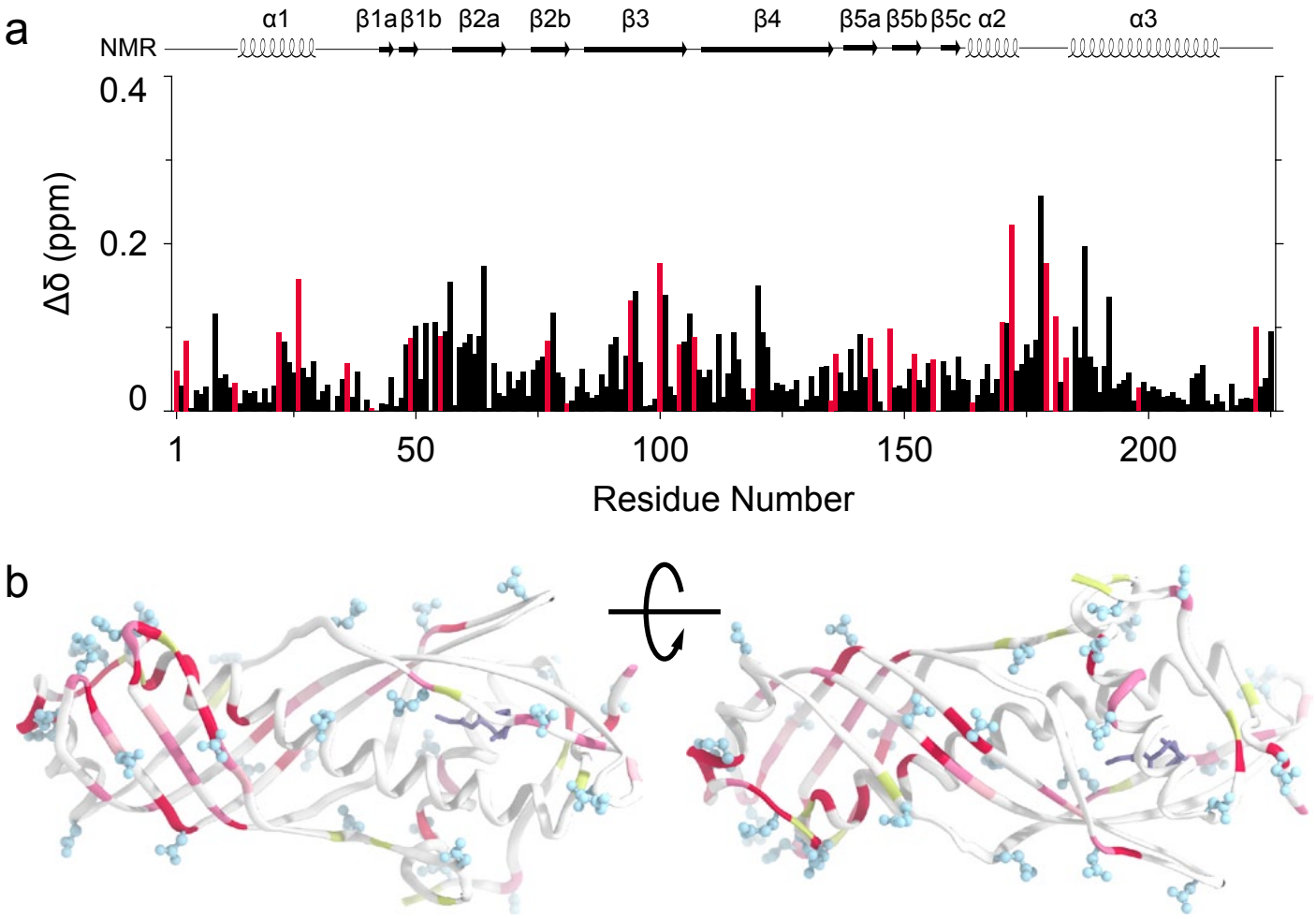


**Supplementary Figure S5 |** (**a**) Comparison of backbone amide $^{1}H$ and $^{15}N$ chemical shifts of the JH III-bound *B. mori* JHBP between pH 6 and pH 4. Weighted chemical shift differences between pH 6 and pH 4, calculated with a function $\Delta\delta = [\Delta\delta_{HN}^{2} + (\Delta\delta_{15N}/5)^{2}]^{1/2}$, are shown against residue number. Red bars represent Asp and Glu residues. The secondary structure elements of the JH III-bound form in solution are presented at the top of the figure. (**b**) Mapping of the perturbed residues of the JH III-bound JHBP upon changing pH from 6 to 4. The perturbed residues shown in red, magenta, and pink are classified according to the magnitude of the perturbation, $\Delta\delta > 0.1$, $0.08 < \Delta\delta < 0.1$, and $0.07 < \Delta\delta < 0.08$ ppm, respectively. It is noteworthy that most of the perturbed residues are solvent-exposed Asp and Glu shown as ball-and-stick models, and their surrounding residues. Proline and N-terminal residues are shown in light-green. The bound JH III molecule is shown as a stick model.

**Supplementary Table S1 | Summary of Data Collection and Refinement Statistics of the Crystal Structures of the JH II-bound and apo-JHBP**

| | Se-Met | JH II | Apo |
|---|---|---|---|
| **Data collection** | | | |
| Space group | $P2_12_12_1$ | $C2$ | $P6_322$ |
| Unit cell parameters | | | |
| *a* (Å) | 54.8 | 164.0 | 90.9 |
| *b* (Å) | 114.8 | 46.8 | 90.9 |
| *c* (Å) | 194.1 | 72.2 | 138.3 |
| β (°) | | 102.5 | |
| Beam Line | PF 17A | PF-AR NE-3 | PF-AR NE-3 |
| Wavelength (Å) | 0.97888 | 1.00000 | 1.00000 |
| Resolution (Å) | 50 - 2.80 ( 2.93 - 2.80 ) | 50 - 2.20 ( 2.28 - 2.20 ) | 50 - 2.20 ( 2.28 - 2.20 ) |
| Total reflections | 406072 | 173801 | 366645 |
| Unique reflections | 30555 (2720) | 24811 (1826) | 17925 (1797) |
| *R*-merge | 0.115 (0.499) | 0.075 (0.312) | 0.059 (0.336) |
| Completeness (%) | 98.4 (88.9) | 90.7 (68.1) | 99.8 (100.0) |
| Average $I/\sigma(I)$ | 24.5 (2.5) | 20.2 (5.2) | 57.3 (11.3) |
| Average redundancy | 13.3 (8.7) | 7.0 (6.1) | 20.5 (10.9) |
| **Structure refinement** | | | |
| Resolution (Å) | | 80.1 - 2.20 ( 2.26 - 2.20 ) | 78.7 - 2.20 ( 2.25 - 2.20 ) |
| *R*-factor | | 0.239 (0.236) | 0.234 (0.221) |
| $R_{free}$-factor[a] | | 0.291 (0.281) | 0.254 (0.263) |
| RMSD from ideal | | | |
| Bond lengths (Å) | | 0.015 | 0.017 |
| Bond angles (°) | | 1.63 | 1.58 |
| Ramachandran plot (%) | | | |
| Favored regions | | 95.4 | 96.5 |
| Allowed regions | | 3.9 | 2.5 |
| Outlier regions | | 0.7 | 1.0 |

[a] $R_{free}$-factors were calculated using 5% of the unique reflections.

**Supplementary Table S2 | Comparison of (ϕ, ψ) angles of the hinge point residues for the movement of the gate α1 helix of *B. mori* JHBP between the apo- and JH II-bound forms in the crystalline state**

| Residue | (φ, ψ) angles | |
|---|---|---|
| | apo-form | JH II-bound form[a] |
| Thr28 | (-71.4°, -31.5°) | (-82.9° ± 6.6°, -9.8° ± 1.5°) |
| Ser29 | (-94.0°, -23.7°) | (-50.0° ± 2.1°, -22.7° ± 12.7°) |
| Lys30 | (-112.0°, -18.3°) | (-120.7° ± 16.5°, 16.7° ± 2.6°) |
| Gly31 | (81.9°, -173.0°) | (97.1° ± 12.9°, 158.0° ± 2.2°) |

[a] Average angles of the two structures in the asymmetric crystal unit.

**Supplementary Table S3 | Statistics of the NMR Solution Structure of the JHBP-JH III Complex**

| NOE restraints | Unique | Ambiguous[a] | Total |
|---|---|---|---|
| Intraresidue | 721 | 1127(527) | 1848 |
| Sequential (\|i – j\| = 1) | 805 | 1603(750) | 2408 |
| Medium range (1 < \|i – j\| < 5) | 733 | 1606(732) | 2339 |
| Long range (\|i – j\| ≥ 5) | 1654 | 3493(1564) | 5147 |
| Total | 4274 | 7468(3212) | 11742 |
| Hydrogen bonds | | 89 | |
| Dihedral angle restraints | | | |
| φ Angles | | 147 | |
| ψ Angles | | 147 | |
| RMSD[b] from mean structure | | Residues 1–225 | |
| Backbone atoms | | 0.32 ± 0.04 Å | |
| All heavy atoms | | 0.64 ± 0.05 Å | |
| Ramachandran plot | | All residues | |
| Favored regions | | 90.3% | |
| Allowed regions | | 7.8% | |
| Outlier regions | | 1.8% | |

[a] Numbers of amiguous NOEs. Numbers of ambiguously assigned peaks are indicated in parentheses.

[b] Root mean square deviation of superimposed atoms, calculated by CYANA.

**Supplementary Table S4 | CHARMm Energies Estimated for L-Shaped Conformations of Isolated JH III**

| | NMR 1 | NMR 2 | X-ray A | Xray B | Extend |
|---|---|---|---|---|---|
| C3-C4 | -52.4 ± 7.8<br>(-54.2 ± 6.2) | -81.4 ± 12.2<br>(-77.1 ± 11.2) | 57.5 (58.0) | 50.5 (52.9) | -118.8 |
| C4-C5 | -56.6 ± 3.2<br>(-53.2 ± 4.7) | -70.5 ± 0.7<br>(-48.0 ± 6.0) | 60.9 (59.1) | 57.0 (76.0) | 177.3 |
| C7-C8 | 113.9 ± 1.0<br>(119.4 ± 5.0) | 112.7 ± 0.7<br>(-114.7 ± 14.0) | -6.5 (-0.3) | -113.9 (-89.5) | -115.0 |
| C9-C10 | -82.4 ± 2.5<br>(-60.0 ± 4.9) | 176.5 ± 0.5<br>(137.5 ± 21.9) | 171.3 (157.8) | -82.1 (-127.0) | 141.7 |
| Energy (kcal/mol) | 46.3 ± 2.2 | 45.3 ± 3.3 | 50.6 | 47.7 | 41.2 |

Coordinates of the JH III molecules in 20 NMR models were used as initial structures for energy minimization calculations of JH III with *gauch*(-) C3-C4 and C4-C5 bonds. The resulted JH III structures are classified into two groups by the torsion angles about the C7-C8 and C9-C10 bonds (1 for 15 structures and 2 for five structures). Two JH II molecules bound to JHBP A and B chains in an asymmetric unit of X-ray structure were energy-minimized and ethyl group bound to epoxy carbon was substituted by methyl group to prepare initial structure of JH III with *gauch*(+) C3-C4 and C4-C5 bonds. An initial structure of extended JH III model was build to have 180° torsion angles for all rotatable bonds. Torsion angles of initial structures are shown in parentheses. The energy minimization calculations were executed with CHARMm forcefield and partial charges estimated by use of MMFF94.